Flat soliton microcomb source

Xinyu Wang, Xuke Qiu, Mulong Liu, Feng Liu, Mengmeng Li, Linpei Xue, Bohan Chen, Mingran Zhang and Peng Xie

---

Related articles

Sub-femtometer-resolution absolute spectroscopy with sweeping electro-optic combs

Bingxin Xu, Xinyu Fan, Shuai Wang, Zuyuan He

Opto-Electronic Advances   2022 **5**, 210023   doi: 10.29026/oea.2022.210023

More related article in Opto-Electron Journals Group website

OE_Journal   Website

Flat soliton microcomb source

Xinyu Wang[1†], Xuke Qiu[2†], Mulong Liu[3†], Feng Liu[2], Mengmeng Li[2], Linpei Xue[2], Bohan Chen[2], Mingran Zhang[4] and Peng Xie[2,5*]

Mode-locked microcombs with flat spectral profiles provide the high signal-to-noise ratio and are in high demand for wavelength division multiplexing (WDM)-based applications, particularly in future high-capacity communication and parallel optical computing. Here, we present two solutions to generate local relatively flat spectral profiles. One microcavity with ultra-flat integrated dispersion is pumped to generate one relatively flat single soliton source spanning over 150 nm. Besides, one extraordinary soliton crystal with single vacancy demonstrates the local relatively flat microcomb lines when the inner soliton spacings are slightly irregular. Our work paves a new way for soliton-based applications owing to the relatively flat spectral characteristics.

Keywords: ultra-flat integrated dispersion; flat spectral profile; soliton microcomb

Introduction

Optical microcavity provides the abundant nonlinear investigations owing to the strong field enhancement. The emergence of optical frequency comb in the high-quality microcavity brings to the optical ruler to chip-scale integration and mode-locking pulse with ultrahigh repetition rate. Dissipative Kerr solitons (DKSs) emerged from the balances of cavity dissipation and gain, as well as nonlinearity and dispersion maintain their temporal waveform during propagating in the Kerr medias[1−6]. This chip-scale optical soliton source is envisioned to play the essential roles in integrated microwave photonics[7], high-speed accurate ranging measurements[8−10], dual-comb spectroscopy[11−13], and optical information processing assisted by wavelength division multiplexing techniques[14−18]. To date, various techniques have been in-

troduced to generate the coherent soliton microcomb sources, including fast frequency tuning[19], power-kicking[20], self-injecting solitons[21], auxiliary modes[22], auxiliary lasers heating the cavity[23], photorefractive effects[24], and extraordinary soliton states[25,26].

Optical amplifier is one fundamental path of adapting the light signal power to the demands of engineering and scientific applications. Signal-to-noise ratio (SNR) is one important criterion for exploring the soliton-based applications when external amplifiers are introduced to enhance the microcomb power. The amplifier spontaneous emission (ASE) can significantly impact the noise level of the microcombs and microcomb lines with lower power are challenging to be utilized. One feasible method is focused on increasing the soliton transformation efficiency, e.g. platicon or dark pulse at the normal

[1]School of Future Technology, University of Chinese Academy of Sciences, Beijing 100049, China; [2]Department of Engineering Science, University of Oxford, Parks Road, Oxford OX1 3PJ, UK; [3]School of Science, Northwest A&F University, Yangling 712100, China; [4]Department of Physics, City University of Hong Kong, Kowloon, Hong Kong 999077, SAR, China; [5]School of Electrical and Electronic Engineering, Nanyang Technological University, Singapore 639798, Singapore.

[†]These authors contributed equally to this work.

*Correspondence: P Xie, E-mail: peng.xie@ntu.edu.sg

dispersion regime[25], periodic or quasi-periodic arranged soliton sequences termed as soliton crystals (SCs)[27], and solitons in coupled dual microcavities[28–30]. However, these strategies still result in the power attenuation when the microcomb lines are far away from the pump laser, all the microcomb lines are still not efficiently used. An alternative approach is constructing one specific solion which is not sensitive to the cavity dispersion or soliton source with large-scale flat spectral profiles. The wide-spread optical source with flat spectral profile is widely prepared in electro-optics modulation combs[31], dispersion-less fiber cavities assisted by dispersion optimization[32], microcomb coherent combining[33], artificial intelligence-driven meta-microcavities[34,35] and micro-cavity with near-zero dispersion characteristics[36,37]. Microcavity with dispersion-less characteristics at a larger wavelength domain could facilitate the soliton with a large-scale, relatively flat spectral profile.

In this paper, we present two schemes for forming a soliton microcomb (SMC) source with the relatively flat spectral envelope. One special microcavity with an ultra-flat integrated dispersion spanning from 1500 nm to 1650 nm is pumped by the counter-propagating dual-color lasers. Single soliton at this dispersion-less regime demonstrates the relatively flat spectral envelope. Besides, microcavity with pure quadratic dispersion also ensures the implementation of local relatively flat spectrum via forming one-defected SC with irregular inter-soliton spacings. Our work not only presents novel soliton dynamics but also offers a high SNR microcomb source, which is crucial for exploring soliton-based applications.

Numerical explorations and experimental results

A numerical model suited to describe the microcomb formation can be modelled by the Lugiato-Lefever equation (LLE)[38]:

$$\frac{\partial A(\Phi, t)}{\partial t} = -\left(\frac{\gamma}{2} + i\delta\right) A(\Phi, t) + i\frac{D_2}{2}\frac{\partial^2 A(\Phi, t)}{\partial \Phi^2}$$
$$+ ig|A(\Phi, t)|^2 A(\Phi, t) + \sqrt{\frac{k_{ex}P_{in}}{\hbar\omega_p}},$$

where Φ is the azimuthal domain along with the circumference of the cavity, t is the evolution time of the field envelope. $A(\Phi, t)$ is the propagating field envelope circulating in the microcavity. γ, $D_2/2\pi$ and P_{in} denote as the total dissipation rate, second-order dispersion and on-

chip power, respectively. g is single-photon-induced Kerr frequency shift. k_{ex} is the external coupling rate between microcavity and waveguide. δ is the cavity detune between the degenerate mode eigenfrequency ω_0 and the pump frequency ω_p. Figure 1 shows the simulated optical spectrum of single SMC under different dispersion conditions. The simulation parameters for the condition of anomalous dispersion regime are set as: input wavelength λ_p=1560 nm, second-order dispersion $D_2/2\pi = 200$ kHz, soliton repetition rate $D_1/2\pi = 200$ GHz, single-photon-induced Kerr frequency shift $g = 1.2$, total quality $Q = 1.5$ million and external quality $Q_{ext} = 6$ million, on-chip pump power 150 mW. When the micro-cavity is located at the anomalous dispersion regime (red line in Fig. 1(b)), a bright soliton with a sech² function profile exhibits a prominent power attenuation with a power variation of approximately 10 dB in the 160 nm range, as shown in Fig. 1(a). As shown in Fig. 1(b), by adjusting the local dispersion to 0 (from the −50th resonance mode to 50th resonance mode), a single soliton microcomb with a local relatively flat spectrum (blue line in Fig. 1(a)) is achieved, demonstrating ~2.5 dB power variation at the same 160 nm wavelength range. Furthermore, we also investigate the spectral envelope of single soliton at the normal dispersion regime in Fig. 1(c). The second-order dispersion ($D_2/2\pi$) is −200 kHz and one frequency shift of −200 MHz on the pump mode is introduced to achieve the local anomalous dispersion. A typical dark platicon is observed with high local power levels (red curve in Fig. 1(c)) but still exhibits the significant power variations in one larger frequency domain. When local integrated dispersion is tuned to zero (from −100th resonance mode to 100th resonance mode as shown in Fig. 1(d)), the stable single soliton (blue line in Fig. 1(c)) has one relatively flat domain with about 320 nm spectrum width. At this region, the maximum power variation is ~6 dB. Meanwhile, temporal waveform of single soliton demonstrates the typical bright pulsed waveform owing to the implementations of large-scale weak anomalous dispersion. The presence of large-scale ultra-flat integrated dispersion promotes the formation of flat solitons, offering the feasibility to achieve the high-SNR microcomb sources when the external amplifier is introduced.

To overcome the strong thermo-optic effect, an auxiliary laser is constructed by using a commercial acoustic optical modulator and an external radio-frequency (RF) signal. Both the pump laser and auxiliary laser are

amplified by using a polarization-maintaining amplifier and counter-coupled in the micro-resonator. The output signals are monitored by using an optical spectrum analyzer (OSA), an electrical spectrum analyzer (ESA), and an oscilloscope (OSC) (Fig. 2(a)). The core device re-

sponsible for microcomb generation is a CMOS-compatible all-pass micro-ring resonator (MRR), fabricated on high-index doped silica glass platform, as is shown in Fig. 2(b). The micro-resonator is coupled with a commercial standard fiber-array with a coupling loss of 3 dB
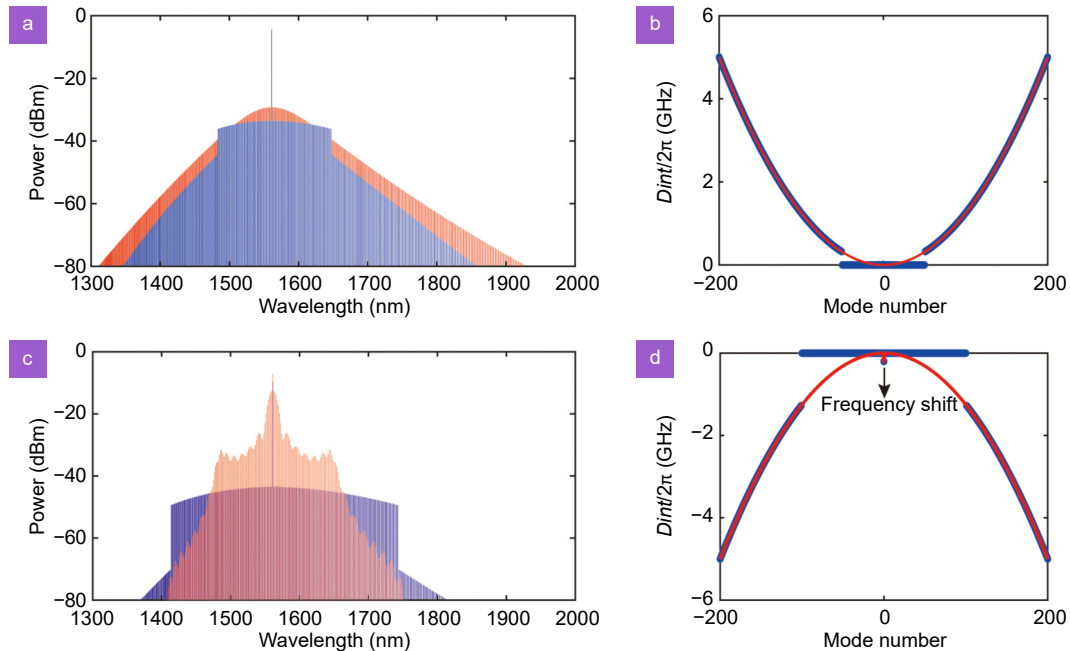

Fig. 1 | Optical spectrums of single SMC source and dispersion curves. (**a**, **c**) and (**b**, **d**) are the simulated optical spectrums of single soliton and dispersion curves, respectively. Blue line and red line in dispersion curves correspond to the conditions of local flat integrated dispersion and initial dispersion. Large-scale flat dispersion reduces the microcomb power variations at the ultra-weak dispersion regime.
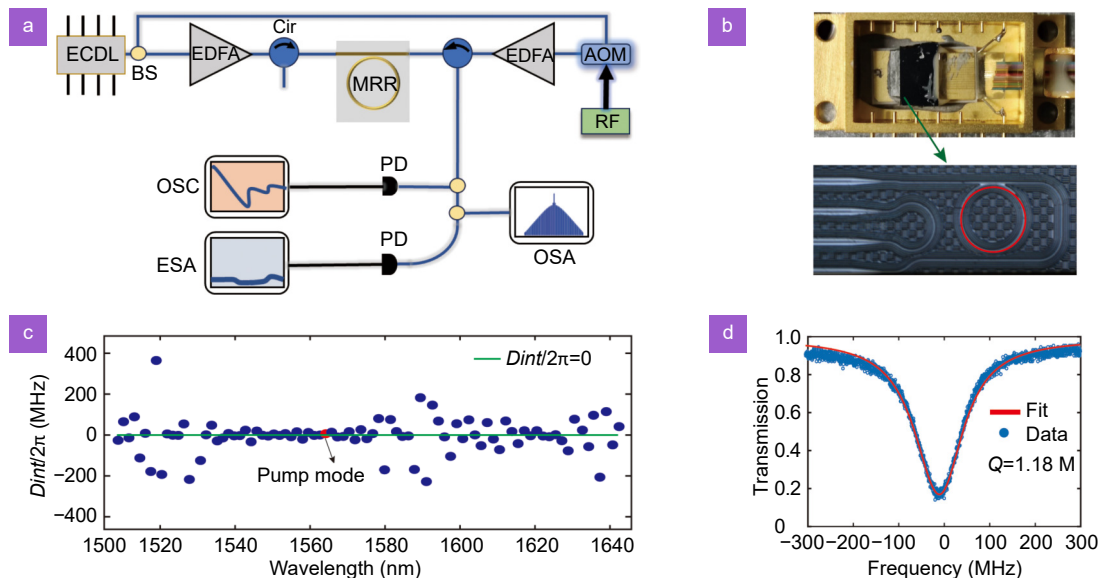

Fig. 2 | Experimental setup. (**a**) Experimental setup for the robust single SMC formation. An auxiliary laser is introduced for the stable soliton formation. ECDL, External cavity diode laser; EDFA, Erbium-doped fiber amplifier; OSA, Optical spectrum analyzer; OSC, Oscilloscope; ESA, Electrical spectrum analyzer; MRR, Micro-ring resonator; PD, Photodetector; Cir, Circulator. (**b**) Microscope image of the high-index doped silica glass micro-ring resonator with a radius of 148.1 μm (lower panel). Butterfly-packaged device (upper panel). (**c**) Dispersion characteristic of the MRR. The green line (*D*int=0) is one referenced integrated dispersion curve. The micro-cavity demonstrates the ultra-flat dispersion characteristic. The red-dot is the soliton mode. (**d**) The transmission spectra of the soliton mode.

per facet. One thermoelectric cooler (TEC) chip is used for temperature stabilization. The MRR has a radius of 148.1 μm and the free spectral range (FSR) is 190 GHz. The dispersion curve is shown in Fig. 2(c). A specific integrated dispersion curve (green line in Fig. 2(c)) serves as one reference, and over 40 modes are closed to the green reference line, indicating an ultra-flat or ultra-weak integrated dispersion characteristic ranging from 1500 nm to 1650 nm. This ultra-flat integrated disper-

sion covers the S, C, and L bands, enabling relatively flat SMC generation across a wide spectral range. The pump mode is marked by a red dot in Fig. 2(c) and has a Q-factor of 1.18 million as shown in Fig. 2(d).

To verify the dynamics of the single SMC evolution in the flat integrated dispersion regime and ensure the implementation of thermal balance, the initial modulation frequency on the acoustic optical modulator (AOM) is set to 100 MHz, and the pump laser wavelength is 1564.2
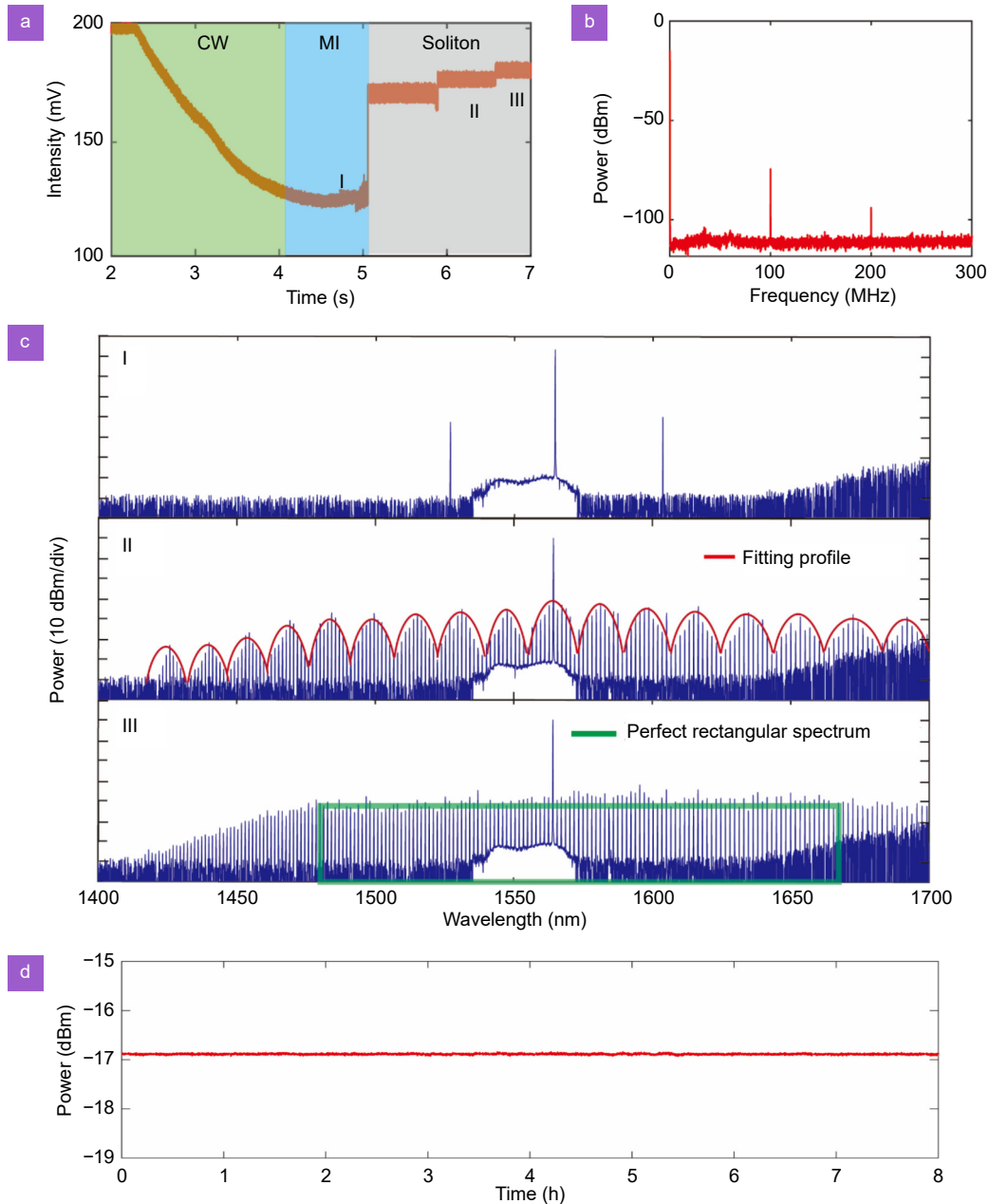

Fig. 3 | Experimental results at the flat dispersion regime. (**a**) Power trace of microcomb evolution from the continuous wave (CW) state to single soliton state. MI: Modulation instability. I: Turning pattern. II: Dual-soliton microcomb. III: Single soliton microcomb. (**b**) Radio frequency spectrum of single soliton state. (**c**) Optical spectrums of Turning pattern (I), dual-soliton microcomb (II) and single SMC source (III). Via introducing the perfect rectangular spectrum as one standard reference, the single SMC demonstrates the trapezoidal spectrum with weak power-varied spectral profile. (**d**) Long-term power trace of single SMC.

nm. The pump laser and auxiliary laser maintain the identical polarization. Figure 3(a) shows the power trace from the continuous wave (CW) state to the single SMC state. Thermal tuning of the operation temperature of microcavity to make the pump laser entry into the resonance mode and the accumulated intra-cavity power gradually meets the threshold of four-wave mixing (FWM) as shown in Fig. 3(c). The first parametric sidebands (state I) are 25-FSR away from the pump. Continuously decrease the operation temperature of the MRR, soliton steps are observed in Fig. 3(a). Once the soliton existence regime is reached, a typical bi-directional tuning technique is employed: the modulation frequency of the AOM is increased, and the pump laser frequency is decreased by using piezoelectric (PZT) control. Typical soliton switching as shown in Fig. 3(a) leads to the generation of a single SMC (Ⅲ) from the dual-soliton microcomb (Ⅱ) with typical dual-pulse interference characteristics in Fig. 3(c). After obtaining a stable single SMC, the modulation frequency on the AOM is backward tuned to 100 MHz to enhance the stability of micro-soliton, and the beat signal is demonstrated in Fig. 3(b). The ideal generated single SMC exhibits a rectangular spectrum, marked by the green line in Fig. 3(c), and the experimental spectrum shows the trapezoidal profile. The power of the spectrum shows some fluctuations due to irregular mode shifts[39]. These fluctuations can be mitigated through better optimization methods in the dispersion curve and loss control, resulting in flatter microcombs. Long-term stability of soliton is of vital import-

ance for exploring soliton-based applications. Figure 3(d) shows the long-term power traces by the feedback on the laser frequency and the single SMC has higher stability toward the environment.

Soliton crystal (SC) is an extraordinary soliton state characterized by collectively ordered soliton sequences, which is known for enhancing the microcomb power due to their high conversion efficiency. The formation of SCs relies on the interference between the modulated background wave and the chaotic modulation instability (MI) field. Intracavity modulated background wave could be constructed by perturbation on the local dispersion. Figure 4 shows the experimental results for SC with local relatively spectral lines. The core device is a high-index doped silica glass MRR, which has a FSR of 48.9 GHz for the fundamental TM mode. The microcavity is designed with anomalous dispersion and has the cross section of 2 μm × 3 μm. Figure 4(a) shows the dispersion curve of TM_{00} mode and the second-order dispersion $(D_2/2\pi)$ is 141.35 kHz. Typical mode-crossing effect is around 1514.4 nm. In our experiments, the wavelength of the pump laser is 1556.4 nm. The spacing between pump laser and mode-crossing mode is 105 FSR. The on-chip power is about 850 mW. Via controlling the operation temperature of microcavity, various SCs could be formed. SCs exhibit various temporal structures, including periodic arranged solitons termed as perfect soliton crystals, vacancies, superstructure and other complex arranged structure. Among these SC states, a specific defected soliton crystal with slight irregular inter-soliton
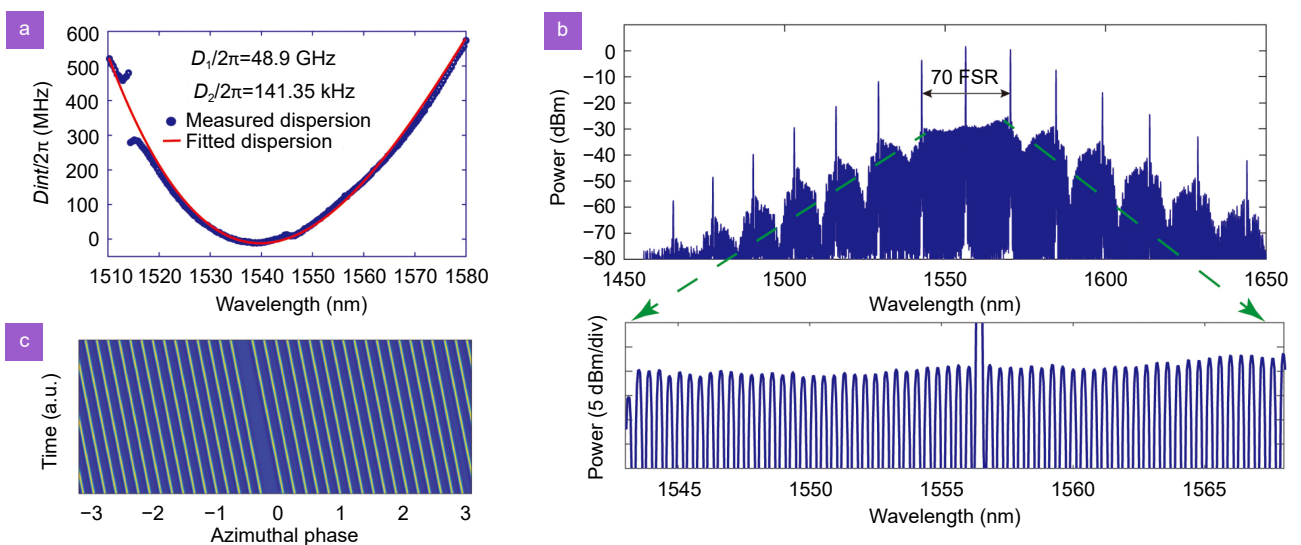

Fig. 4 | Experimental results for SC formation with local relatively flat spectrum. (**a**) Dispersion characteristic of microcavity. (**b**) Soliton crystal with irregular inter-soliton spacings. Zoom-in local spectrum. At this frequency region, the microcomb demonstrates the relatively flat spectral profile. (**c**) Temporal evolution of SC with local relatively flat spectral lines.

spacings provides the local flat spectral lines, as shown in Fig. 4(b). In this case, 34 solitons stably exist in the micro-cavity as shown in Fig. 4(c), and the local flat spectral range covers approximately 25 nm. The local perturbations of microcomb power in this type of SC are mainly induced by different dissipation rates and Raman-induced frequency shifts[40]. This specific SC can be converted from a soliton crystal with one defect by slightly tuning the operation temperature or laser frequency[41].

Conclusion

In conclusion, we have demonstrated two methods for generating the coherent mode-locked microcomb source with the local relatively flat spectral profile in the microring resonator. One micro-cavity with large-range ultra-flat integrated dispersion is verified and single SMC at this ultra-flat dispersion regime demonstrates relatively flat spectral lines from 1480 nm to 1650 nm, effectively covering the S, C, and L bands. Besides, we explore the generation of local flat microcomb lines using a single-defected soliton crystal with slightly irregular soliton spacing. This WDM-compatible flat soliton microcomb is an excellent candidate as multi-wavelength source for parallel high-capacity informational processing and parallel photonic neuromorphic computing.

References

1. Akhmediev N, Ankiewicz A. *Dissipative Solitons* (Springer, Berlin, Heidelberg, 2005).
2. Chang L, Liu ST, Bowers JE. Integrated optical frequency comb technologies. *Nat Photonics* **16**, 95–108 (2022).
3. Gaeta AL, Lipson M, Kippenberg TJ. Photonic-chip-based frequency combs. *Nat Photonics* **13**, 158–169 (2019).
4. Kippenberg TJ, Gaeta AL, Lipson M, Gorodetsky ML. Dissipative Kerr solitons in optical microresonators. *Science* **361**, eaan8083 (2018).
5. Runge AFJ, Hudson DD, Tam KKK, de Sterke CM, Blanco-Redondo A. The pure-quartic soliton laser. *Nat Photonics* **14**, 492–497 (2020).
6. Grelu P, Akhmediev N. Dissipative solitons for mode-locked lasers. *Nat Photonics* **6**, 84–92 (2012).
7. Marpaung D, Yao JP, Capmany J. Integrated microwave photonics. *Nat Photonics* **13**, 80–90 (2019).
8. Riemensberger J, Lukashchuk A, Karpov M, Weng WL, Lucas E et al Massively parallel coherent laser ranging using a soliton microcomb. *Nature* **581**, 164–170 (2020).
9. Suh MG, Vahala KJ. Soliton microcomb range measurement. *Science* **359**, 884–887 (2018).
10. Trocha P, Karpov M, Ganin D, Pfeiffer MHP, Kordts A et al. Ultrafast optical ranging using microresonator soliton frequency combs. *Science* **359**, 887–891 (2018).
11. Suh MG, Yang QF, Yang KY, Yi X, Vahala KJ. Microresonator

12. Dutt A, Joshi C, Ji XC, Cardenas J, Okawachi Y et al. On-chip dual comb source for spectroscopy. *Sci Adv* **4**, e1701858 (2018).
13. Xu BX, Fan XY, Wang S, He ZY. Sub-femtometer-resolution absolute spectroscopy with sweeping electro-optic combs. *Opto-Electron Adv* **5**, 210023 (2022).
14. Raja AS, Lange S, Karpov M, Shi K, Fu X et al. Ultrafast optical circuit switching for data centers using integrated soliton microcombs. *Nat Commun* **12**, 5867 (2021).
15. Feldmann J, Youngblood N, Karpov M, Gehring H, Li X et al. Parallel convolutional processing using an integrated photonic tensor core. *Nature* **589**, 52–58 (2021).
16. Xu XY, Tan MX, Corcoran B, Wu JY, Boes A et al. 11 TOPS photonic convolutional accelerator for optical neural networks. *Nature* **589**, 44–51 (2021).
17. Wang XY, Xie P, Chen BH, Zhang XC. Chip-based high-dimensional optical neural network. *Nano-Micro Lett* **14**, 221 (2022).
18. Rizzo A, Novick A, Gopal V, Kim BY, Ji XC et al. Massively scalable Kerr comb-driven silicon photonic link. *Nat Photonics* **17**, 781–790 (2023).
19. Herr T, Brasch V, Jost JD, Wang CY, Kondratiev NM et al. Temporal solitons in optical microresonators. *Nat Photonics* **8**, 145–152 (2014).
20. Yi X, Yang QF, Yang KY, Suh MG, Vahala K. Soliton frequency comb at microwave rates in a high-*Q* silica microresonator. *Optica* **2**, 1078–1085 (2015).
21. Shen BQ, Chang L, Liu JQ, Wang HM, Yang QF et al. Integrated turnkey soliton microcombs. *Nature* **582**, 365–369 (2020).
22. Li Q, Briles TC, Westly DA, Drake TE, Stone JR et al. Stably accessing octave-spanning microresonator frequency combs in the soliton regime. *Optica* **4**, 193–203 (2017).
23. Wang XY, Xie P, Wang WQ, Wang Y, Lu ZZ et al. Program-controlled single soliton microcomb source. *Photonics Res* **9**, 66–72 (2021).
24. He Y, Yang QF, Ling JW, Luo R, Liang HX et al. Self-starting bichromatic LiNbO$_3$ soliton microcomb. *Optica* **6**, 1138–1144 (2019).
25. Xue XX, Xuan Y, Liu Y, Wang PH, Chen S et al. Mode-locked dark pulse Kerr combs in normal-dispersion microresonators. *Nat Photonics* **9**, 594–600 (2015).
26. Bruch AW, Liu XW, Gong Z, Surya JB, Li M et al. Pockels soliton microcomb. *Nat Photonics* **15**, 21–27 (2021).
27. Cole DC, Lamb ES, Del'Haye P, Diddams SA, Papp SB. Soliton crystals in Kerr resonators. *Nat Photonics* **11**, 671–676 (2017).
28. Boggio JMC, Bodenmüller D, Ahmed S, Wabnitz S, Modotto D et al. Efficient Kerr soliton comb generation in micro-resonator with interferometric back-coupling. *Nat Commun* **13**, 1292 (2022).
29. Xue XX, Zheng XP, Zhou BK. Super-efficient temporal solitons in mutually coupled optical cavities. *Nat Photonics* **13**, 616–622 (2019).
30. Helgason ÓB, Girardi M, Ye ZC, Lei FC, Schröder J et al. Surpassing the nonlinear conversion efficiency of soliton microcombs. *Nat Photonics* **17**, 992–999 (2023).
31. Parriaux A, Hammani K, Millot G. Electro-optic frequency combs. *Adv Opt Photonics* **12**, 223–287 (2020).
32. Xue XX, Grelu P, Yang BF, Wang M, Li SY et al. Dispersionless Kerr solitons in spectrally confined optical cavities. *Light Sci Appl* **12**, 19 (2023).

33. Kim BY, Okawachi Y, Jang JK, Ji XC, Lipson M et al. Coherent combining for high-power Kerr combs. *Laser Photonics Rev* **17**, 2200607 (2023).

34. Meng Y, Chen YZ, Lu LH, Ding YM, Cusano A et al. Optical meta-waveguides for integrated photonics and beyond. *Light Sci Appl* **10**, 235 (2021).

35. Lucas E, Yu SP, Briles TC, Carlson DR, Papp SB. Tailoring microcombs with inverse-designed, meta-dispersion microresonators. *Nat Photonics* **17**, 943–950 (2023).

36. Xiao ZY, Li TY, Cai ML, Zhang HY, Huang Y et al. Near-zero-dispersion soliton and broadband modulational instability Kerr microcombs in anomalous dispersion. *Light Sci Appl* **12**, 33 (2023).

37. Anderson MH, Weng WL, Lihachev G, Tikan A, Liu JQ et al. Zero dispersion Kerr solitons in optical microresonators. *Nat Commun* **13**, 4764 (2022).

38. Godey C, Balakireva IV, Coillet A, Chembo YK. Stability analysis of the spatiotemporal Lugiato–Lefever model for Kerr optical frequency combs in the anomalous and normal dispersion regimes. *Phys Rev A* **89**, 063814 (2014).

39. Herr T, Brasch V, Jost JD, Mirgorodskiy I, Lihachev G et al. Mode spectrum and temporal soliton formation in optical microresonators. *Phys Rev Lett* **113**, 123901 (2014).

40. Lu ZZ, Wang WQ, Zhang WF, Liu ML, Wang LR et al. Raman self-frequency-shift of soliton crystal in a high index doped silica micro-ring resonator [Invited]. *Opt Mater Express* **8**, 2662–2669 (2018).

41. Wang WQ, Lu ZZ, Zhang WF, Chu ST, Little BE et al. Robust soliton crystals in a thermally controlled microresonator. *Opt Lett* **43**, 2002–2005 (2018).

Acknowledgements

Author contributions

XY Wang, XK Qiu and P Xie conceived this concept. All authors contributed to the manuscript. P Xie supervised the whole project.

Competing interests

The authors declare no competing financial interests.